

## The zooming and homogenizing laser illumination system for shortwave infrared imaging

CHEN Da-Ming<sup>1,2</sup>, LI Yong-Fu<sup>1\*</sup>, WANG Yu-Rong<sup>2</sup>, FEI Cheng<sup>1,2</sup>, FANG Jia-Xiong<sup>1</sup>

(1. Advanced Research Center for Optics, Shandong University, Jinan 250100, China;  
2. School of Information Science and Technology, Shandong University, Jinan 250100, China)

**Abstract:** Recent years, shortwave infrared (SWIR) imaging system has been developed rapidly, and additional active lighting is very necessary in some scenarios. At present, the uniformities of laser illumination homogenization schemes commonly used are not high, and can't reach the requirements of imaging. A new 25 × zoom laser illumination system was designed based on the analysis of the laser model in fiber and the theory of zoom illumination system. The optical lens of the illumination system is composed of three groups of lenses, and the CAM structure achieves continuous zooming. This system is small in size, has simple structure, and gains large zoom ratio. Finally a continuous change of 2 ~ 50° in illumination angle is achieved. Laser illumination intensity uniformity reaches 92.7%. In the imaging experiments, the human identify distance was up to 1.2 km. The continuous zoom laser illumination system is of high significant for improving the ability of the short-wave infrared night vision system.

**Key words:** Infrared and night vision technology, shortwave infrared imaging, laser illumination, laser uniformity, zoom lens

**PACS:** 85.60.Bt #2.15.Eq #2.60.By

## 短波红外成像变焦匀化激光照明系统

陈大明<sup>1,2</sup>, 李永富<sup>1\*</sup>, 王玉荣<sup>2</sup>, 费成<sup>1,2</sup>, 方家熊<sup>1</sup>

(1. 山东大学 光学高等研究中心, 山东 济南 250100;  
2. 山东大学 信息科学与工程学院, 山东 济南 250100)

**摘要:** 针对近年来得到迅速发展的短波红外成像系统, 分析了增加激光主动照明的必要性. 目前常用的激光照明匀化方案均匀性均不高, 达不到照明成像的要求. 提出了连续变焦激光照明系统, 使用成像镜头把光纤端面的像直接成像在被照明表面, 照明光斑均匀. 分析了变焦照明系统的设计理论, 设计了 25 倍变焦的短波红外激光照明系统. 该照明系统的光学镜头由 3 组镜片组成, 由凸轮结构实现连续变焦. 体积小, 结构简单, 变焦倍数大. 最终实现了 2 ~ 50° 的照明角度连续变化. 照明光斑均匀度达到 92.7%. 进行了野外成像实验, 对人员识别距离可达 1.2 km. 设计的连续变焦激光照明系统对提高短波红外成像系统的夜视能力具有较高的意义.

**关键词:** 红外与夜视技术; 短波红外成像; 激光照明; 激光匀化; 变焦系统

中图分类号: TN216 文献标识码: A

### Introduction

In recent years, with the development of semicon-

ductor technology, a kind of high quantum efficiency short-wave infrared solid imaging technology is being more and more attention response<sup>[1]</sup>. InGaAs array detectors operating in the 0.9 to 1.7 μm wavelength range

**Received date:** 2017-10-27, **revised date:** 2018-01-04

**收稿日期:** 2017-10-27, **修回日期:** 2018-01-04

**Foundation items:** Supported by the Opening Foundation of Key Laboratory of Infrared Imaging Materials and Devices and in part by the Shanghai Institute of Technical Physics, CAS (IIMDKFJJ-16-08)

**Biography:** CHEN Da-Ming (1980-), male, Jinan Shandong, Ph. D. candidate. Research interests are shortwave infrared imaging systems and active laser illumination imaging systems. E-mail: chendaming@mail.sdu.edu.cn

\* **Corresponding author:** E-mail: yfli@sdu.edu.cn

have been proved to be the most practical for imaging applications due to their high quantum efficiency and low dark current at room temperature. This short-wave infrared focal plane imaging system based on the InGaAs photoelectric device is likely to fully replace the night vision goggles and visible light imaging system. The short-wave infrared imaging system is able to fill the blank from the visible light to medium wave infrared spectrum, and has many advantages, such as: imaging through the glass, using optical glass lens, good ability to penetrate the fog, better using of the night sky light, etc. [2-4]

But under certain conditions, such as: in cloudy night, underground or in the outer space, etc., environmental short-wave infrared light can't meet the requirements of imaging. Another situation is long distance night imaging, while long focal length lens are using generally. The telephoto lens can't have the same large relative aperture as short focal lens, so the F/number of telephoto lens is commonly above 4. These cause the system loss of ability to receive the ambient light, or the detector can't meet the imaging energy conditions. Under these conditions, the use of laser active illumination can improve the image quality of InGaAs focal plane array (FPA), and get a better image contrast. Laser illumination optical system has two main requirements: speckle homogenization and angle control.

## 1 Several kinds of common laser illumination technology

In order to match the spectral region of an InGaAs photoelectric device, active laser illumination imaging systems generally use a solid or semiconductor laser as a light source with a wavelength of 1.06  $\mu\text{m}$  or 1.55  $\mu\text{m}$ . The coherence of the laser is higher, so when the laser is used as a lighting source, the laser emission angle can be easily controlled, but at the same time it brings serious laser speckle faults. The laser spot forms shadows and white spots on the imaged image. These spots can reduce the resolution of the imaging system.

In recent years, different laser lighting schemes have been designed to achieve better illumination effects, such as: special aspheric lens technology, micro lens array technology, single lens, diffraction optics technology, etc. The aspherical lens technology modulates the Gaussian laser beam into a flat distribution through a plano-concave aspherical lens and a plano-convex aspheric lens, and the laser beam achieves uniform illumination. It was proposed by Frieden, mainly for single-mode laser beam, with high energy conversion rate, good aesthetic effect, arbitrary wavefront transformation and coaxial distribution, but this complex aspherical processing has certain technical difficulties [5]. Microlens arrays use arrayed optical elements to achieve uniform illumination. The incident laser light is divided into sub-beams by the lens array, and then the sub-beams are superimposed on the target surface. The splitting of the beam and the superposition of the sub-beams eliminate the influence of the non-uniformity of the incident laser distribution and achieve uniform illumination of the target surface [6]. There is a gap in the array and Fresnel diffraction occurs at the edge of the microlens, so some of the laser energy

is lost. Single-lens technology places the positive lens in place away from the end of the fiber. This lens reduces the output angle of the fiber and directs the alignment. These can improve focusing efficiency and reduce energy loss. This method can change the angle of light but does not improve the quality and uniformity of light [7]. Diffractive optical elements (DOEs) have many features that traditional optical elements do not [8], such as spot configurability, miniaturization, arraying, and integration. Diffractive optical elements are finely processed, so the quality is limited by the level of development of fine processing technology.

**Table 1 The comparison of existing illumination systems**

表 1 现有照明系统的比较

Technology	Advantage	Disadvantage
Special aspheric lens	High efficiency, Good uniformity	Production difficulties, Mainly for single-mode fiber, No zooming
Micro lens array	Good uniformity	Loss of energy, No zooming
Single lens	Changing the angle of the light (zooming)	Nonuniformity
Diffraction optics	Configurable adumbration of the facula, miniaturization	Production difficulties, No zooming

The advantages and disadvantages of the existing lighting system are shown in Table 1. These illumination systems typically maintain a portion of Gaussian and laser speckle, resulting in global and local inhomogeneities in the laser spot. Most laser lighting technologies cannot change the size of the spot, and thus are not conducive to the cooperation with the zoom imaging lens.

## 2 Zooming and homogenizing laser illumination system design

### 2.1 Homogenization of multimode fibers

Illumination source is laser diode array (LDA). The laser output of the diode array beams is coupled into a multimode optical fiber, and then output from the other end of the optical fiber. According to the mode theory of optical fiber transmission, the optical energy is distributed in accordance with the mode. There are mode coupling and mode conversion in multimode fiber. After reaching the equilibrium length, there is a stable power distribution on the fiber end face. Most of the optical power is concentrated in the basic mode and low order mode concentrated in steady state [9]. The relationship between the fiber core diameter  $2a$  and the conduction mode number  $M$  is described as follows:

$$M = 2 \left( \frac{\pi a}{\lambda} \right)^2 (n_1^2 - n_2^2) \quad , \quad (1)$$

$n_1$  and  $n_2$  are the refractive index of the fiber core and cladding, respectively. At the output end, the superposition of the light field along the radial distribution can be described by the Gauss function [10]:

$$I(r, z) = \frac{I_0}{\omega_3^2(z)} \exp \left[ -\frac{2r^2}{\omega_3^2(z)} \right] \quad , \quad (2)$$

where  $\omega_3^2(z)$  is the beam radius. The output light field of multimode optical fiber was measured using the method of lateral migration<sup>[11]</sup>. In the short distance ( distance less than 0.05 mm) , the emission intensity is approximately uniform in the fiber core diameter , and the intensity of the long distance is Gauss distribution.

In this paper , the design of the short wave infrared zoom illumination system is the first time to apply the zoom imaging technology in the field of laser illumination. Because of the imaging of the optical fiber end surface , the near field image of the fiber end is obtained on the target. The illumination optical system is a zoom lens , so that the spot size on the target can be changed continuously , and the illumination spot with different divergence angle and variable intensity could be obtained. According to the principle of the zoom imaging system , the illumination system schematic diagram is shown in Fig. 1.

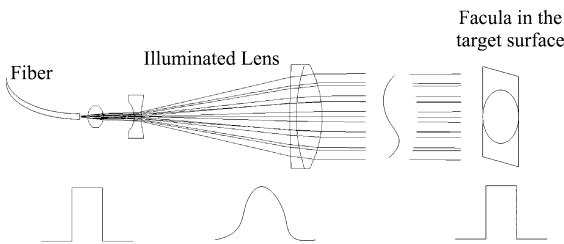


Fig. 1 Short wave infrared zoom illumination system  
图 1 短波红外变焦照明系统

**2.2 Theoretical analysis of zoom illumination system**

The semiconductor laser wavelength of the illumination system is 1.55  $\mu\text{m}$  , the power is 4 W , the core diameter of the output optical fiber is 200  $\mu\text{m}$  , and the numerical aperture ( NA) of the fiber is 0.22. The focal length of the imaging lens is 20 ~ 500 mm , the resolution of the imaging device is 320\* 240 , and the pixel size is 30  $\mu\text{m}$ . The field of view of the illumination system is consistent with the imaging system , so the focal length of the illumination system can be calculated by the following formula , and the focal length is 0.4 ~ 10 mm. Zoom ratio is 25 times.

$$f_i = f_L \frac{A_L}{A_F} \quad (3)$$

In Eq. (3) ,  $f_i$  is the focal length of the illumination system ,  $f_L$  is the focal length of the imaging lens ,  $A_L$  is the fiber core diameter , and  $A_F$  is the image size of the imaging device.

The zoom illumination system is designed to the optical system without anterior fixation group. The first group is the positive power lens , the second group is the negative power lens. The axial movement of the two groups changes the focal length. The movement of the middle group ( group second) is linear , while movement of the front lens is nonlinear , which is used to maintain the stability of the image plane. For the mechanically compensated zoom optical system with two moving elements , the kinematic relationship between the zoom group and the compensation group can be calculated:

$$Aq_2^2 + Bq_2 + C = 0 \quad (4)$$

where

$$\begin{cases} A = (f_2' - \beta_1 q_1) \beta_2 \\ B = \beta_1 \beta_2 q_1^2 + [f_3' (1 - \beta_2^2) \beta_1 - f_2' (1 - \beta_1^2) \beta_2] \\ \quad q_1 - f_2' f_3' (1 - \beta_2^2) \\ C = \beta_2^2 f_3' [\beta_1 q_1 - f_2' (1 - \beta_1^2)] q_1 \end{cases} \quad (5)$$

The motion variables of the compensation group are obtained:

$$q_2 = \frac{-B \pm \sqrt{B^2 - 4AC}}{2A} \quad (6)$$

where  $\beta_1$  is the lateral magnification of the zoom group at the initial position ,  $\beta_2$  is the lateral magnification of the compensation group at the initial position ,  $q_1$  indicates the displacement of the zoom group along the optical axis ,  $q_2$  indicates the displacement of the compensation group along the optical axis ,  $f_2'$  is the focal length of the zoom group , and  $f_3'$  is the focal length of the compensation group<sup>[12]</sup>.

The focal length of the zoom group , compensation group , post fixation group and the distance between the groups were calculated by Gauss optics. In view of the miniaturization of zoom optical system , after repeated calculation and comparison , the final focal length of each group is as follows: the focal length of the zoom group is 45.5 mm , the focal length of the compensation group is -4.77 mm , travel of the zoom group is 43.9 mm , and Compensation is 18.9 mm.

**2.3 Design of zoom illumination system**

The aberration of this illumination zoom system is different from that of the imaging system. The image plane size is small , so the aberrations are mainly axial. Since the laser irradiation wavelength is single , there is no color difference. Therefore , the system mainly considers axial aberrations , amplification factors , and ensures that the curve has no breakpoints.

In addition , the zoom illumination system is also different from the imaging system in terms of aberrations. The integrated aberrations of the imaging system are generally considered , and the system's modulation transfer function ( MTF) is as small as possible. Distortions and other aberrations will not affect the image quality. But for the aberrations of the illumination system , spherical aberration , coma aberration , astigmatism and astigmatism affect the light field distribution of the illumination spot , resulting in the image edges becoming brighter or weaker ( see Fig. 2) . Therefore , these deviations should be optimized.

The illumination system is optimized by using optical design software. Because the object distance of this system is far less than image distance , optical design uses reverse path. The optical path and the cam curve is shown in Fig. 3. The optical parameters obtained are as listed in Table 2.

**2.4 Aberration analysis of zoom illumination system**

Because the laser illumination wavelength is single , the chromatic aberration isn't considered. There are the modulation transfer function ( MTF) of long-focus , mid-focus , and short-focus ( from top to bottom , as shown in

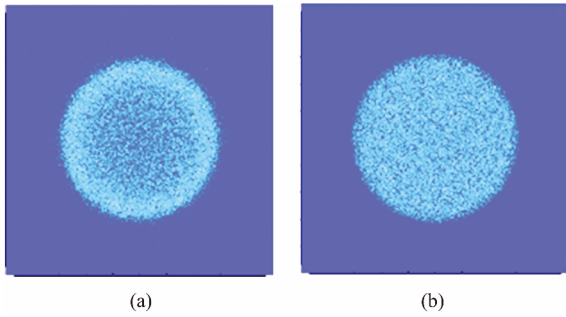


Fig.2 The influence of the aberration on the distribution of illumination spot. (a) more astigmatism in the edge field of view , (b) less astigmatism in the edge field of view

图2 像差对照明光斑分布的影响 (a) 边缘视场有较大像散 (b) 边缘视场无像散

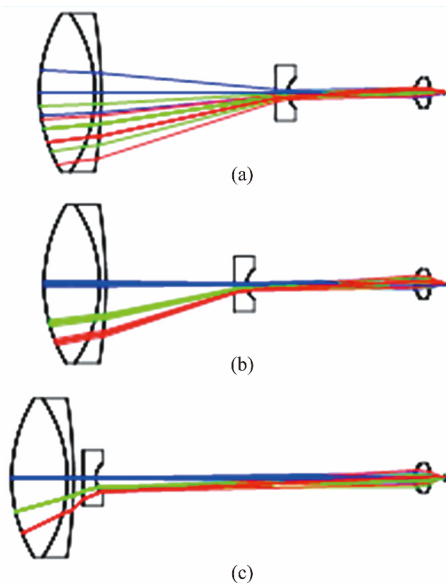


Fig.3 light path of zoom illumination system ( a ,b and c are different focal length)

图3 变焦照明系统光路图( a,b,c 分别为长焦 ,中焦和短焦光路)

Fig.4) , corresponding to small laser spot , middle laser spot , and large laser spot. On the right side of Fig. 4 , the far field spot distributions of different focus are simulated in optical design software. The light intensity distribution is uniform in the far field spot.

Table 2 Illuminated lens data ( Unit: mm)

表2 照明镜头参数( 单位: mm)

Surface Number	Type	Radius	Thickness	Glass	Semi-Diameter
0	STANDARD		Infinity		0.00
1	STANDARD	26.66	6.00	H-ZK9A	12.00
2	STANDARD	-39.26	1.50	H-ZLAF50B	12.00
3	STANDARD	-225.72	33.84		12.00
4	STANDARD	-17.3	1.50	H-ZLAF50B	4.50
5	STANDARD	5.012	7.06		3.50
6	STANDARD	3.232	3.70	H-ZLAF50B	2.00
7	STANDARD	-3.232	1.50		2.00
8	FIBER		0.00		0.1

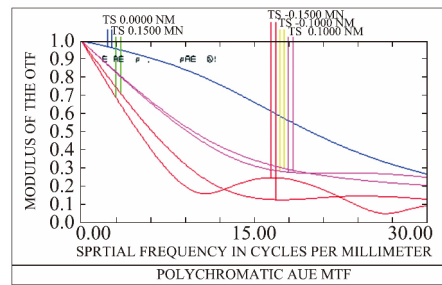
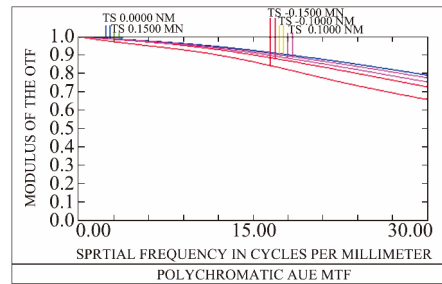
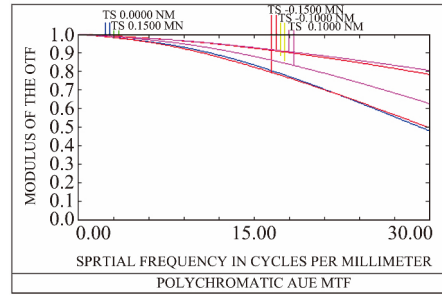


Fig.4 Aberration zoom illumination system and simulated spot

图4 照明系统像差

### 3 Experiment and uniformity calculation

After the design of the illumination system , the spot test was carried out in the laboratory. The picture of the system was shown in Fig.5. The picture of the spot on the far field target was photoed using short wave infrared imaging system ( as shown in Fig. 6 ( a ) , at the telephoto end) . When the target is 10 m away , the spot size is 0.2 m. The spot is uniform , and has a clear edge , however the spot of single lens illumination system for the contrastive study ( as shown in Fig. 6 ( b ) ) has obvious dark ring , Gaussian-like distribution , and poor uniformity.

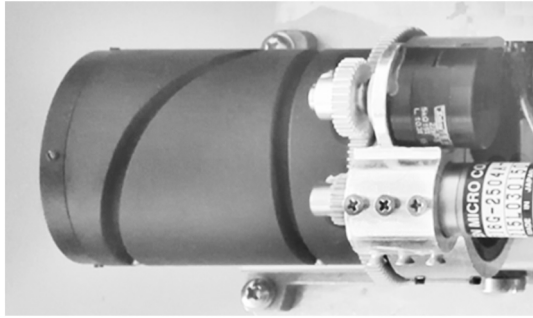


Fig. 5 Physical object of the illumination system  
图 5 照明系统实物

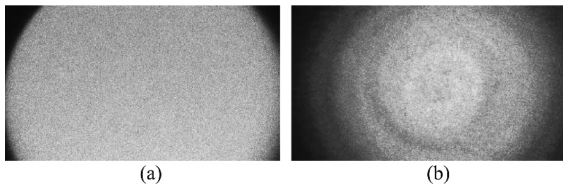


Fig. 6 Test spot in the laboratory ( target distance: 10 m , spot size: 0.2 m ). ( a ) zoom illumination system , ( b ) single lens illumination system  
图 6 实验室测试光斑图(目标距离 10 m ,照明光斑 0.2 m) ( a ) 变焦照明系统 ( b ) 单透镜照明系统

The uniformity of light spot can be defined by the following:

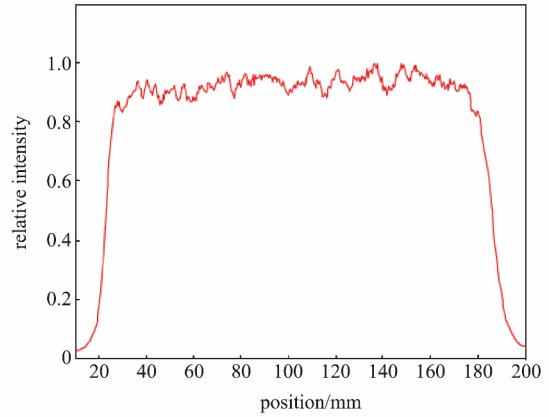
$$C = 1 - \frac{I_{\max} - I_{\min}}{I_{\max} + I_{\min}} \quad (7)$$

where  $I_{\max}$  is the maximum light intensity in the spot and  $I_{\min}$  is the minimum light intensity. According to Fig. 7, C can be calculated. The spot uniformity of the zoom illumination system at telephoto end is 92.7%, therefore the uniformity of light spot in conventional single lens illumination system is just 33.2%. Using the same method, the spot and the light distribution section diagram of mid-focal and the wide-angle end( as shown in Fig. 8). The spot uniformity of the zoom illumination system at mid-focal is 87.6%, and it's 81.7% at the wide-angle end, because of the remaining aberration.

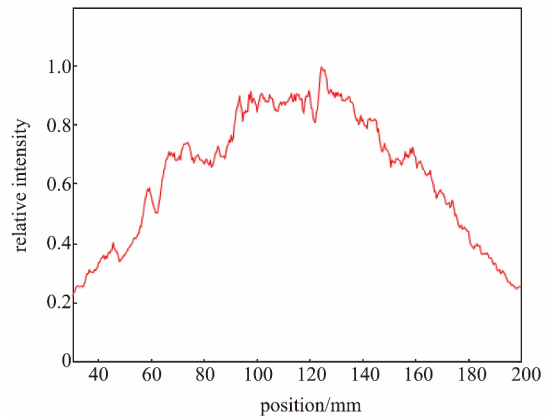
After completing the spot test in the laboratory, the short wave infrared active imaging system is set up to carry out the field test, using the imaging system( mentioned in Sect. 2.2) and the short wave infrared zoom illumination system. The air temperature was 20°C and the visibility was 8km. At night without starlight, the 500 m, 1200 m targets are imaged individually ( as shown in Fig. 9). The spot sizes were 30 m and 20 m. The image is clear and the spot is uniformity. Because of the high contrast, the building and human goals can be identified.

### 4 Conclusions

Based on the theory of continuous zoom and the distribution of laser modes in multimode fiber, a continuous zoom short wave infrared illumination system is designed,

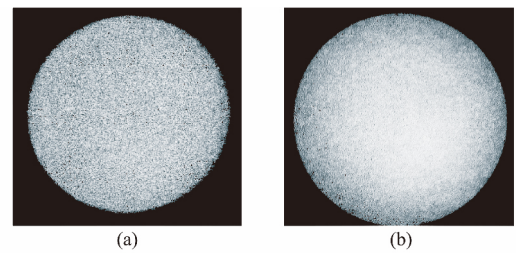


(a)



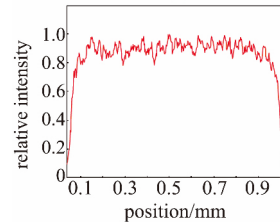
(b)

Fig. 7 Section diagram of light distribution( a ) zoom illumination system, ( b ) single lens illumination system  
图 7 光强分布剖面图( a ) 变焦照明系统 ( b ) 单透镜照明系统

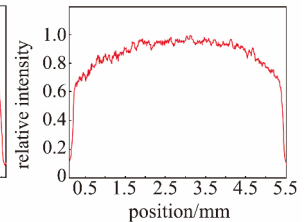


(a)

(b)



(c)



(d)

Fig. 8 spot and light distribution of mid-focal/ wide-angle ( a ) the spot of mid-focal ( b ) the spot of the wide-angle end, ( c ) light distribution of mid-focal, ( d ) light distribution of the wide-angle end

图 8 中焦距和广角的光斑和光强分布 ( a ) 变焦照明系统中焦光斑 ( b ) 变焦照明系统广角光斑 ( c ) 变焦照明系统中焦光斑 ( d ) 变焦照明系统广角光斑

which uses 3 groups of lenses to realize that the illumina-



Fig.9 pictures of field target experiment ( target distance: 500 m , 1200 m)

图9 野外目标实验图像

tion angle changes 25 times. Laser illumination intensity uniformity reaches 92.7%. In the imaging experiments, the human identify distance was up to 1.2 km. Good illumination results were obtained. The zoom illumination lens of the active imaging systems has the advantages of simple structure, uniform spot, and that spot angle can change continuously. It provides a good illumination scheme for active short wave infrared imaging system.

## References

[1] Marc P Hansen, Douglas S Malchow. Overview of SWIR detectors, cameras, and applications [J]. *SPIE*, 2008, **6939**: 1-11.

- [2] Borniol E De Guellec, F Castelein P. High-performance 640 × 512 pixel hybrid InGaAs image sensor for night vision [C]. *SPIE*, 2012, **8353**: 8353-05.
- [3] Nichter J E, Martin T J, Onat B M, et al. Develop multipurpose In-GaAs focal plane array visible/SWIR camera for staring and range-gated applications [C]. *SPIE*, 2007, **6572**: 657201.
- [4] Richard A. IR Imaging Optics Meet Varied Needs [J]. *Photonics Spectra*, 2012, **46**(8): .
- [5] Frieden B R. Lossless conversion of a plane laser wave to a plane wave of uniform irradiance [J]. *Appl. Opt.*, 1965, **4**(11): 1400-1403.
- [6] Sales R. M. . Structured microlens arrays for beam shaping [J]. *Proceedings of SPIE*. 2003, **5175**: 109-110.
- [7] WANG Ying-shun, LIAN Jie, GAO Shang, WANG Xiao, SUN Zhao-zong. Illumination Uniformity of Near Infrared Illuminator [J]. *Acta Photonica Sinica*, 2013, **42**(3): 258-261.
- [8] Hirai T, Fuse K, Kurise, K. . Development of diffractive beam homogenizer [J]. *Sei Technical Review*, 2005, **60**: 17-23.
- [9] YUAN Li-bo. Light source and the optical field formed by an optical fiber [J]. *Optical Communication Technology*, 1994, **18**(1): 54-64.
- [10] LI Ai-yun, WANG Xiao-ying. Study on Optical Properties of Fiber Bundle Coupling LD Output Beams [J]. *ACTA P HOTONICA SINICA*, 2007, **36**(9): 1664-1667.
- [11] QI Xiao-ling, WANG Fu-juan, CAI Zhi-gang, et al. Intensity distribution of transmitted beam of multimode optical fiber [J]. *Semiconductor Optoelectronics* 2003, **24**(2): 117-120.
- [12] DU Yu-nan, MU Da, LIU Ying-ying, WANG Wen-sheng. Design of 20 × Long Wavelength Infrared Zoom Optical System. *Infrared Technology* [J], *Infrared Technology*, 2013, **35**(10): 607-611.

(上接第 277 页)

As can be seen from the table, when the heating power is 49.7 W, the temperature of the cathode emitter ring is about 1070°C, while the surface temperature simulated by ANSYS software is 1134°C. The relative error is lower than 6% between the simulation result and experiment data.

## 4 Conclusion

Thermal analysis of the W-band gyrotron traveling wave electron gun is carried out by using finite element software ANSYS. The temperature distribution and thermal deformation of the cathode component are obtained when the heating power of the filament heater is 45 W. The temperature of the cathode emitter ring is about 1070°C. The maximum thermal deformation of the cathode surface is 0.102 mm under this temperature. By using EGUN software, the performance of the electron beam with and without the deformation is not changed very much. Finally, thermal analysis results are compared with experimental values. It turns out that simulation results are consistent with experiment results.

## References

[1] Barker R J, Schamiogil E. *High-Power Microwave Sources and Technol-*

- ogies* [M]. Piscataway, NJ: IEEE, 2001.
- [2] Thumm M. , State-of-the-art of high power gyro-devices and free electron masers update 2011 KIT Scientific Reports 7606. [EB OL] <http://uvka.ubka.uni-karlsruhe.de/shop/download>.
- [3] Chu K R. The Electron Cyclotron Maser [J]. *Rev. Modern Phys.* 2004, **76**: 489-540.
- [4] McDermott D B, Song H H, Hirata Y, et al. Design of a W-band TE<sub>01</sub> mode gyrotron traveling-wave amplifier with high power and broad-band capabilities [J]. *IEEE Trans. Plasmas Sci.*, 2002, **30**(3): 894-902.
- [5] Felch K L, Danly B G, Jory H R, et al. Characteristics and applications of fast-wave gyrodevice [J], *Proc. IEEE*, 1999, **87**: 752-781.
- [6] Nguyen K T, Calame J P, Pershing D E, et al. Design of a Ka-Band Gyro-TWT for Radar Applications, *IEEE Trans. Electron Devices*, 2001, **48**(1): 108-115.
- [7] Lawrence R. Ives, Philipp Borchard, George Collins, et al. Improved Magnetron Injection Guns for Gyrotrons [J]. *IEEE Transaction on Plasma Science*, 2008, **36**(3): 620-629.
- [8] Nguyen K T, Danly B G, Levuch B, et al. Electron gun and collector design for 94 GHz gyro-amplifiers [J]. *IEEE Trans. Plasma Science*, 1998, **26**(3): 799-813.
- [9] Gilmour A S, Klystrons Jr. *Traveling Wave Tubes, Magnetrons, Crossed-Field Amplifiers, and Gyrotrons* [M]. Artech House, 2011: 583-626.
- [10] Yang shiming, Tao wenquan, *Heat Transfer* [M] 4rd, Higher Education Press, 2006.
- [11] Reference Manual for ANSYS 10.0 [M], ANSYS Inc.